

25 such as rough postural assessment, time and motion study or trajectory analysis where some errors in motion
26 data would not significantly sacrifice their reliability. Combined with relatively accurate angular
27 measurement sensors, vision-based motion capture approaches also have great potential to enable us to
28 perform in-depth physical demand analysis such as biomechanical analysis that requires full-body motion
29 data, even though further improvement of accuracy is necessary. Additionally, understanding of body
30 kinematics of workers would enable ergonomic mechanical design for automated machines and assistive
31 robots that help to reduce physical demands while supporting workers' capabilities.

32 **Keyword:** Body Kinematics, Motion Capture, Construction

33 **INTRODUCTION**

34 Construction workers are frequently exposed to excessive physical demands in a relatively dangerous and
35 unhealthy working environment that may lead to health and safety issues [1]. Despite recent improvements
36 by adopting best practices (e.g., tool box meetings and structured hazard analysis processes) to deal with
37 these issues, the construction sector still remains as one of the hazardous industries, showing higher rates
38 of fatal and nonfatal injuries than other industries [2]. Consequently, evaluating and controlling physical
39 demands from the job, equipment and environment not to exceed one's capabilities is essential to prevent
40 and mitigate potential health and safety risks.

41 In-depth evaluation and control of physical demands should begin with measuring body kinematics that
42 include body position, displacement, velocity and acceleration [3]. Human motions not only create loads
43 on the involved musculoskeletal system (e.g., muscles and tendons) by themselves or combined with
44 external forces, but they also have an important role in accompanying an action by transmitting forces
45 generated from a body (i.e., active muscle contraction) to the external environment [4]. As a result,
46 kinematics data can provide contextual information on the fundamental causes of changing physical
47 demands as a worker's behavior is affected by physical work environmental factors (e.g., geometry of the
48 workplaces, temperature, and types of tools), as well as individual factors (e.g., anthropometry and

49 preferred working techniques) [5]. Also, enhanced awareness of body kinematics of workers helps to
50 support effective design of automated machines and assistive robotics that can not only reduce physical
51 demands from work, but also enhance workers' capabilities by improving ergonomics in human-machine
52 (or robot) interaction [6,7]. Such an understanding of workers body kinematics would also inform
53 contemporary research in construction ergonomics and robotics, given current developments in architecture,
54 gerontechnology, exoskeletons, anthropomorphic robotics, augmented reality, and industrialized
55 construction environments because they all demand highly interdependent and integrated kinematics
56 systems solutions [9-15].

57 Generally, measuring body kinematics is enabled by using motion capture techniques that are based on
58 optical, inertial, mechanical, magnetic or acoustic approaches. Among them, optical motion capture systems
59 are the most popular solution to obtain 3D full-body motion data by tracking active or passive markers
60 attached to the body. They have been widely used for diverse applications including clinical motion analysis
61 and biomechanical study. Despite their precision and reliability, their applications in practice have been
62 limited due to the need for complex laboratory settings, the high cost of devices and the time consuming
63 procedure for data collection. Their most critical drawback is the need for simulating tasks in a controlled
64 environment by assuming that captured motions correspond to typical activities under real conditions [8].
65 However, considering the continuously changing and unstructured nature of working environments in
66 construction, it is hard to simulate construction tasks in a controlled setting by reflecting all possible
67 situations that would exist on sites. As a result, an effective and easily accessible means for collecting in-
68 field motion data at construction sites is required to evaluate potential safety and health risks of workers
69 while performing tasks.

70 Recently, vision-based (i.e., markerless) motion capture approaches have gained interest. These approaches
71 appear to be promising as an in-field motion data collection method by addressing some of the major
72 challenges that exist with optical motion capture systems. For example, as these vision-based approaches
73 obtain body kinematics data by processing 2D or 3D images directly collected from real conditions, they

74 don't need complex laboratory settings or markers attached to a human body. Also, 2D or 3D images can
75 be collected using any type of existing ordinary video cameras or affordable 3D image sensing devices (e.g.,
76 RGB-D sensors and stereovision cameras). The ease of use, non-invasiveness and cost-effectiveness of
77 vision-based approaches can broaden the spectrum of their applications for job analysis under real
78 conditions. Additionally, the use of body fixed sensors such as Inertial Measurement Units (IMUs) or
79 angular measurement sensors (e.g., goniometers, optical encoders, strain gauges or magnetic sensors) has
80 provided effective solutions for in-field motion measurement [8]. Combined with a wireless data
81 transmission capability, these approaches allow us to obtain real-time motion data. For 3D full-body
82 kinematic measurements, several commercialized IMU-based (e.g., XsensTM (Xsens North America Inc.,
83 xsens.com)) or mechanical (e.g., Gypsy 7TM (Meta Motion, metamotion.com)) motion capture systems are
84 available, but the need for wearing a full-body suit equipped with sensors may interfere with on-going work.
85 Instead, wearing light-weight and wearable angular measurement sensors attached only at a specific body
86 joint of interest may minimize workers' discomfort during performing tasks, though they only provide one
87 degree of freedom joint angle.

88 To measure workers' body kinematics non-invasively or minimally invasively at construction sites, both
89 vision-based and angular measurement sensor-based approaches are viable means, although several
90 limitations such as sensitivity to self-occlusions (i.e., occlusions of specific body joints by other body parts)
91 of vision-based approaches and limited use of angular measurement sensors still remain [8,16-18]. Given
92 the pros and cons of these approaches, an in-depth understanding of the performance of each approach can
93 lead to better decisions for appropriate uses of these approaches in construction.

94 With this background, this paper reports on the evaluation of motion data obtained from vision-based and
95 angular measurement sensor-based approaches through an experimental study. Specifically, three emerging
96 vision-based approaches for collecting motion data during construction tasks are selected. Those are: 1)
97 RGB-D sensor-based [17]; 2) stereo-vision camera-based [19]; and 3) multiple camera-based [16,18]
98 approaches. An optical encoder, which is a potentiometer-based electro-goniometers [20], is applied as an

99 angular measurement sensor. Also, a marker-based motion capture system (Optotrak™, Northern Digital,
100 Inc., Waterloo, Canada) is used as the ground truth of motion data. To compare the accuracy of motion data,
101 selected joint angles from each approach are compared with the ones from Optotrak™ during performance
102 of several dynamic tasks. Based on the results, the performance of these approaches and their potential
103 application areas for analyzing construction tasks are discussed.

104

105 **STATE-OF-THE-ART IN IN-FIELD BODY KINEMATICS MEASUREMENTS**

106 This section describes technical aspects and procedures of the state-of-the-art approaches that enable us to
107 non-invasively or minimally invasively measure body kinematics while workers perform tasks at
108 construction sites. Those include: 1) vision-based approaches, and 2) angular measurement sensor-based
109 approaches. Also, by reviewing previous work on these approaches, the pros and cons of each approach are
110 summarized.

111 **Vision-based Motion Capture Approaches**

112 Vision-based approaches aim to extract full-body motion data by processing 2D or 3D images [21].
113 Previous research efforts have developed several vision-based approaches: 1) RGB-D sensor-based [17,
114 22-25]; 2) stereo-vision camera-based [19, 53]; and 3) multiple camera-based [16,18] approaches. While
115 RGB-D sensor- and stereovision camera-based approaches take an advantage of the 3D imaging sensors
116 that directly provide 3D information on scenes, a multiple camera-based approach relies on photogeometric
117 acquisition of 3D body joint locations (i.e., 3D reconstruction) from tracked 2D joint locations of multi-
118 view images.

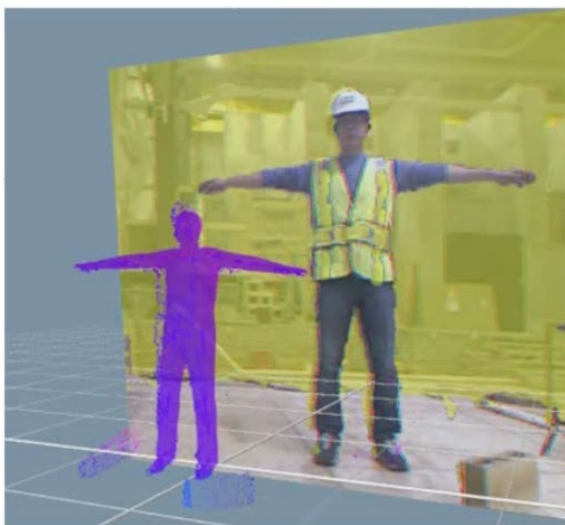
119 *RGB-D sensor-based approach*

120 Several computer vision algorithms have been developed to estimate human poses by detecting the 3D
121 positions of body joints directly from RGB-D images [22-25]. Recently, motion capture solutions such as

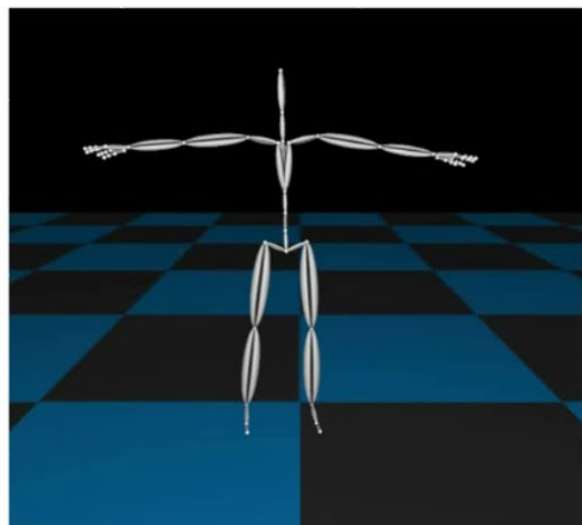
122 iPi Desktop Motion Capture (www.ipisoft.com) and OpenNI (www.openni.org) that use a Microsoft Kinect
123 sensor have provided effective solutions for extracting skeleton-based motion data from 3D images
124 obtained by RGB-D sensors.

125 The Kinect sensor that was initially developed for video gaming is capable of providing both depth and
126 color information at the resolution of 640×480 and the rate of 30 frames per second [26]. This sensor is
127 equipped with the infrared (IR) projector, the color camera and the IR camera. Using the projected
128 structured IR lights, it measures the depth, reconstructing 3D scenes with point cloud [27]. Combined with
129 the 3D sensing feature of the Kinect, the iPi Desktop Motion Capture software provides a marker-less
130 solution for collecting full-body motion data. Figure 1 shows an example of an RGB-D image with a pre-
131 defined body model, and the corresponding motion data. Basically, the algorithm in this software is model-
132 based, which means that motion data can be tracked by matching the surface of a pre-defined body model
133 with a depth image (Figure 1A). Then, the tracked motion data can be exported into any types of motion
134 data formats such as the Biovision Hierarchy (BVH) motion data (Figure 1B). This software also provides
135 several post-processing algorithms to refine tracking and filtering algorithms for noise removal and
136 smoothing.

A. RGB-D Image with a Body Model



B. Skeleton-based Motion Data (.BVH)



137
138
139

Figure 1. RGB-D Sensor (i.e., Kinect™)-based Motion Capture

140 The following are advantages of an RGB-D sensor-based motion capture approach: 1) no need for markers
141 or sensors attached to human body, which allows for motion capture without interfering with on-going work;
142 2) low cost (e.g., approximately 150 – 250 USD); 3) an easy-to-use and easy-to-carry means for in-field
143 motion data collection [17]. Technically, this approach is robust to self-occlusions because the iPi software
144 provides an inverse kinematics algorithm that can adjust incorrectly tracked body parts due to occlusions.
145 However, as the Kinect uses IR light, the use of this approach is limited only in an indoor environment due
146 to its sensitivity to sunlight. Also, the short operating range of the Kinect sensor (within 4 m) is one of the
147 disadvantages of this approach.

148 Stereovision camera-based approach

149 A stereovision system is designed to extract 3D information from a stereo image pair [28]. Stereo vision
150 works in a similar way to 3D sensing in human vision. It begins with identifying image pixels that
151 correspond to the same point in a physical scene observed by multiple cameras. The 3D position of a point
152 can then be established by triangulation using a ray from each camera. The more corresponding pixels
153 identified, the more 3D points that can be determined with a single set of images. Correlation stereo methods
154 attempt to obtain correspondences for every pixel in the stereo image, resulting in tens of thousands of 3D
155 values generated with every stereo image. A Bumblebee XB3™ manufactured by Point Grey Technologies
156 (www.ptgrey.com) is one of the widely used stereovision cameras. The stereo camera measures line-of-
157 sight distance using two lenses with a narrow baseline in a self-contained unit. This allows for both optical
158 and depth data to be collected with few environmental restrictions (e.g. outdoor environments) and limited
159 field-of-view.

160 Starbuck et al. [19] proposed a stereovision camera-based motion capture approach that addresses the short
161 operating range of an RGB-D sensor. The 3D point cloud data collected from the stereovision camera was
162 converted into a format used by an existing kinematic modeling software solution (i.e., iPi Motion Capture
163 software) designed for use with RGB-D sensors. Then, using the same algorithm used in a RGB-D sensor-
164 based approach, skeleton-based motion data was extracted from the 3D point cloud data. Through a

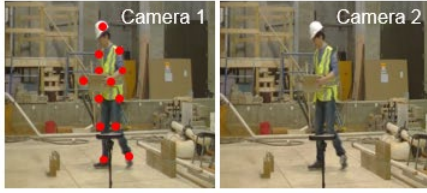
165 laboratory test, the proposed method was proved to be comparable to the traditional RGB-D sensor-based
166 approach [19].

167 A stereovision camera-based approach provides additional advantages, beyond the benefits from the RGB-
168 D sensor-based approach. For example, the use of this approach does not suffer from environmental
169 conditions, allowing both indoor and outdoor applications. Also, the operating range of the stereovision
170 camera is flexible according to lens field-of-view, lens separation, and image size [29]. However, as
171 computing depth information from two images is a computationally intensive task, the frame rate relies on
172 the performance of hardware [29].

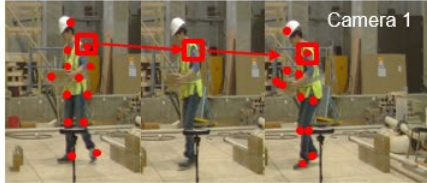
173 Multiple camera-based approach

174 A multiple camera-based motion capture approach aims to estimate the 3D locations of body joints by
175 processing 2D images from two different views using multiple video cameras or a 3D camcorder that has
176 two lenses in one camera [16]. Han and Lee [16] proposed a motion capture process that consists of: 1) 2D
177 pose estimation from one view of images; 2) correspondence matching of body joints on the other view of
178 images; and 3) 3D reconstruction of body joints using the corresponding joint locations identified. However,
179 this approach suffered from the need for extensive training images to detect joint locations on testing images,
180 and significant computation time for 2D pose estimation. To address this issue, Liu et al. [18] modified Han
181 and Lee [16]'s approach by proposing body joint tracking that accelerates the 2D pose estimation process
182 without the prior knowledge (training images for joint detection). Figure 2 shows an overview of the
183 modified approach.

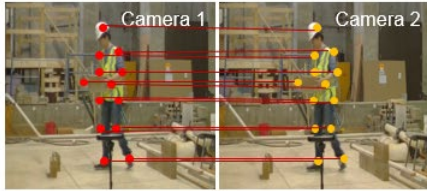
A. Initialization



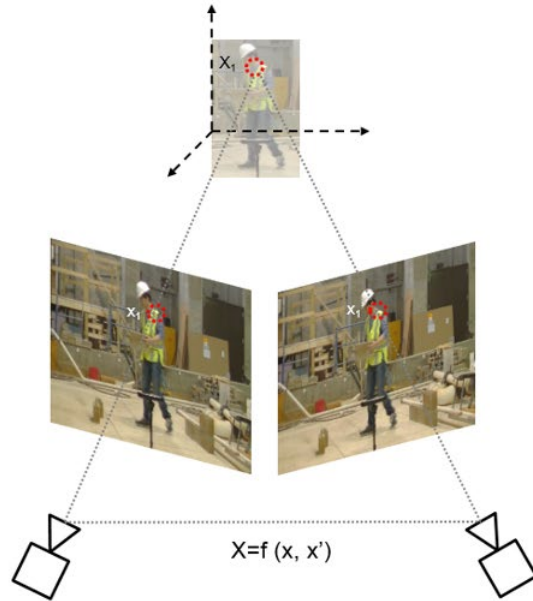
B. Body Joint Tracking



C. Correspondence Matching



D. 3D Reconstruction



184

185

186

Figure 2. An Overview of a Multiple Camera-based Motion Capture Approach

187

The main idea of 2D joint tracking is that continuous tracking of body joints on consecutive image frames

188

enables fast estimation of 2D skeletons [18]. Once the target joints are initialized in the first frame (Figure

189

2A), the algorithm tracks the joints in consecutive images by detecting the image patch with the most similar

190

color histogram with that of the initialized target. To reduce computation time, a modified particle filter

191

tracker was applied to specify a number of reliable candidates for the targets in the subsequent frames [30].

192

The tracking of different body joints is performed independently, resulting in a 2D skeleton model (Figure

193

2B). The next process is to identify the corresponding body joints on the image from the other viewpoint

194

by comparing the features of a pixel with the feature descriptors such as SIFT (Scale-Invariant Feature

195

Transform) [31] and SURF (Speeded Up Robust Features) [32,33] (Figure 2C). To obtain more reliable

196

corresponding locations of body joints, the search space is constrained by epipolar geometry [34] and

197

homography [16]. Once pairs of corresponding body joints are detected from two different viewpoints of

198

images, a 3D reconstruction algorithm detects the 3D positions of each joint through triangulation, resulting

199 in 3D full-body skeleton-based motion data as shown in Figure 2D. Camera intrinsic and extrinsic
200 parameters required for 3D reconstruction are obtained by using Zhang [35]’s camera calibration technique.

201 The strength of a multiple camera-based motion capture approach is that we can use ordinary video cameras
202 to obtain motion data, and thus this approach is less hardware dependent than RGB-D sensor- and
203 stereovision camera-based approaches. Also, it is not only cost effective, but also we can benefit from zoom
204 lenses that collect video images from a distance. Even though environmental conditions such as
205 illuminations may affect the performance of 3D skeleton extraction, post image processing enables us to
206 obtain clear images even in a noisy environment. From previous studies that investigated the accuracy of
207 this approach, about ± 10 cm of errors in body length and up to 20 degrees of errors in joint rotation angles
208 have been reported [16,18]. These errors came from either incorrectly detected joint locations or inaccurate
209 camera calibration process. Especially, the performance of this approach was significantly affected by
210 frequent self-occlusions of forearms (e.g., elbows and hands), which led to larger errors [16,18].

211 **Angular Measurement Sensor-based Approaches**

212 Angular measurement sensor-based approaches directly measure joint angles using sensors attached to
213 specific body joints without the need for any mathematical transformation in space or time. Examples of
214 sensors include goniometers and strain gauges.

215 Goniometers

216 Goniometers have been used to measure joint range of motion. Traditional goniometers were made of a
217 mechanical compass that measures the static relative angle between two body segments [36]. Modern
218 goniometers are made of an electrical compass (potentiometer-based) which can measure static and
219 dynamic relative angles [36,37]. The potentiometer changes its resistance with the rotation of the two body
220 segments connected to it. The principle of operation is that the voltage drop (V) across the potentiometer
221 due to a constant electric current (I) passing through it will depend on the resistance (R) following Ohm’s
222 law:

223
$$V = IR \quad (1)$$

224 Calibration of the potentiometer (goniometer) from 0° to a full range of motion is conducted once to produce
225 a calibration chart that describes the relationship between the change in joint angle and the measured voltage.
226 The use of potentiometer allows for detection of rotary motion as well as for placement of the sensor at
227 center of joint rotation.

228 Strain gauges

229 Strain gauges work on the same principles as goniometers except that the sensing element in a strain gauge
230 responds to translation (change in length (ΔL)) represented as change in resistance (ΔR):

231
$$\Delta R/R = \Delta L/L \quad (2)$$

232 Measuring the joint angle depends on the placement of the strain gauge with respect to the axis of joint
233 rotation [38]. Misalignment can produce significant errors due to the complexity of placing a translational
234 sensor to detect rotatory motion [39].

235

236 **EXPERIMENTAL COMPARISON OF IN-FIELD MOTION CAPTURE APPROACHES**

237 The section describes an experimental test to compare the accuracy of three vision-based motion capture
238 approaches and one angular measurement sensor-based approach: 1) an RGB-D sensor-based approach; 2)
239 a stereovision camera-based approach; 3) a multiple camera-based approach; and 4) an optical encoder (i.e.,
240 a potentiometer-based electrogoniometer).

241 **Testing Conditions**

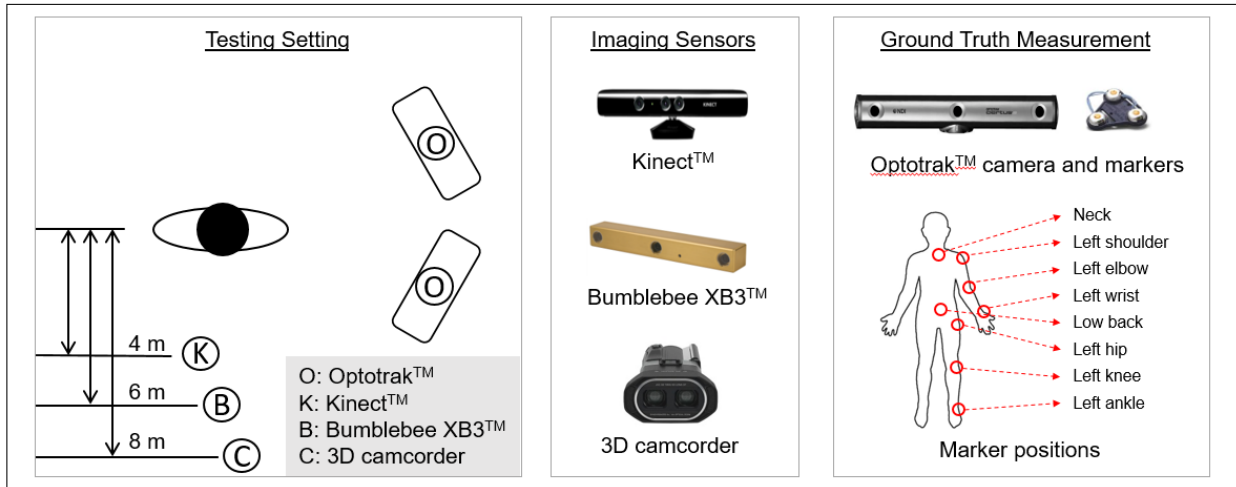
242 Vision-based motion capture approaches and an angular measurement sensor-based approach were tested
243 through two independent testing sessions as shown in Figure 3. An exoskeleton is used to align the optical
244 encoder with the knee flexion axis of rotation. The straps used to attach the exoskeleton to the lower limb

245 were indistinguishable from the subject's clothes and skin. As a result, they could affect performance of
246 image processing for the vision-based approaches, especially the multiple camera-based approach that
247 tracks body joints using color information. To avoid this, the angular measurement sensor-based approach
248 was tested in a separate session from the vision based approaches.

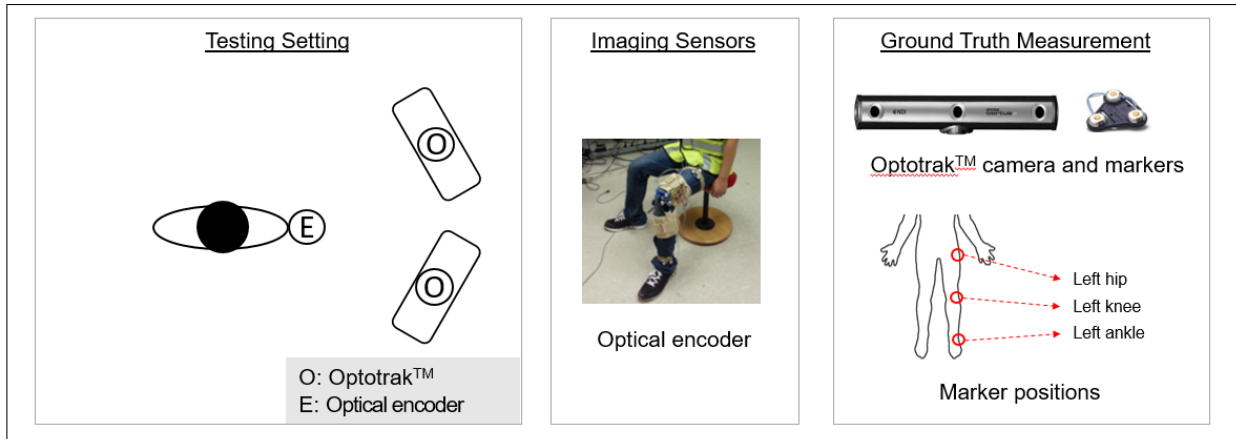
249 Figure 3 shows experimental conditions for each testing session. In the session for vision-based approaches
250 (Figure 3A), three image sensors were located in front of a subject to collect 2D or 3D images from a front
251 view. The Kinect™ (640×480 resolution with 30 frames per second (fps)), Bumblebee XB3™ stereovision
252 camera (320×240 resolution with about 10 fps) and 3D camcorder (1920×1080 resolution with 29 fps) were
253 positioned 4, 6 and 8 meters away from the subject, respectively. The positions of the Kinect™ and
254 Bumblebee XB3™ were determined based on the optimal operating distance proposed by the manufacturer.
255 As the 3D camcorder has zoom lenses, its position was selected to obtain a clear view of the subject's whole
256 body. Motion data obtained from an Optotrak™ system served as a ground truth. The Optotrak™ uses
257 active markers attached on the center of body joints to track body motions. If the markers are captured by
258 at least one of cameras, the system can provide accurate 3D positions of the markers with an accuracy of
259 up to 0.1 mm. The markers were attached to the subject's center and left body joints, including neck, low
260 back, shoulder, elbow, wrist, hip, knee and ankle joints. Two Optotrak™ cameras were positioned to the
261 left side of the subject to prevent possible data loss due to occlusions of the markers.

262 In the session for the angular measurement sensor-based approach (Figure 3B), the optical encoder (550
263 samples per second) was positioned across the left knee to measure knee-included angles, the optical
264 encoder was placed using a specially designed exoskeleton described in [37], reducing the effect of soft
265 tissue movements. To obtain ground truth angles, active markers were attached to left hip, left knee and left
266 ankle joints. Two Optotrak™ cameras were also positioned to the left side of the subject.

A. Testing Session for Vision-based Approaches



B. Testing Session for an Angular Measurement Sensor-based Approach



268
269
270

Figure 3. Experimental Settings and Testing Devices

271 In each session, human motion was simultaneously recorded with these devices. For the synchronization of
272 motion data, the subject was asked to hold a T-pose at the beginning of the recording. Data synchronization
273 was manually performed by identifying the T-pose frame across all measurement techniques.

274 Testing Tasks

275 To compare the accuracy of motion data for diverse tasks, one male subject simulated three types of tasks
276 as shown in Figure 4: 1) basic tasks with movements of specific body parts; 2) lifting and placing; and 3)
277 walking. The basic tasks were designed to test the measurement accuracy for simple motions that involve

278 movements of specific body parts. Those include arm-raising to the front and the side, elbow-bending,
 279 back-bending, back-twisting and knee-bending, which are also common motions in manual work such as
 280 construction. For more dynamic motions involving coordinated body movements, a lifting and placing task
 281 was selected (also common in construction). Specifically, the subject was asked to simulate the lifting task
 282 by lifting an imaginary object from the ground and placing it to the side. Lastly, a walking task was intended
 283 to test the measurement accuracy for rapid repetitive movements. To perform identical tasks for two
 284 independent sessions, the subject was asked to practice the task in question for several times before
 285 recording two test sessions.

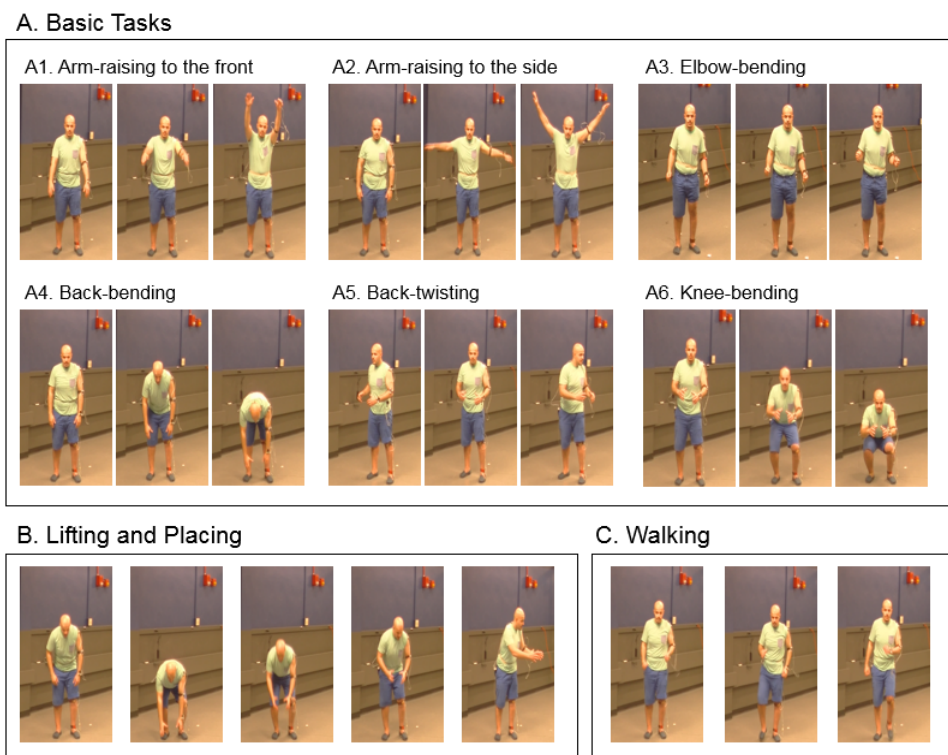


Figure 4. Testing Tasks

286
 287
 288
 289

Measures for Accuracy Comparison

290 As measures of motion data accuracy for vision-based motion capture approaches, previous studies have
 291 used 3D positions of body joints, body link lengths or joint rotation angles [16-19]. However, due to the
 292 difference in body models used in each vision-based approach, the use of these measures may lead to bias

293 in accuracy comparison. For example, joint locations and corresponding body link lengths in a multiple
294 camera-based approach can be calculated based on the measured joint locations of the subject. On the other
295 hand, the RGB-D sensor- and stereovision camera-based approaches capture motions by matching 3D point
296 clouds with a pre-defined body model, and thus the body link length from the captured motion data is
297 affected by anthropometric mismatch between the model and subject. Also, while both RGB-D sensor- and
298 stereovision camera-based approaches provide motion data in a BVH file format that defines body postures
299 using joint rotational angles, these angles are not available in the motion data from the multiple camera-
300 based approaches used in this test [16, 18].

301 To address this issue, the authors define new body angles that are available from all vision-based approaches
302 as shown in Figure 5. Specifically, the body angles of each body part were defined as the angles between
303 the vector of the body segments and the vertical vector. For example, the vector of the upper arm is obtained
304 using 3D shoulder and elbow locations, and the angle between the vector of the upper arm and the vertical
305 vector (y-axis) is calculated as an upper arm (i.e. shoulder) angle. The other body angles such as lower arm
306 (i.e., elbow), trunk flexion, upper leg (i.e., hip) and lower leg (i.e., knee) angles are calculated using the
307 same method. However, the trunk axial rotation angle that indicates how much the back is twisted was
308 computed by using shoulder and hip vectors that were projected onto x-y plane. As the motion data from
309 the three vision-based approaches and OptotrakTM provides 3D locations of body joints, all these angles can
310 be calculated using vectors defined by two selected 3D joint locations, enabling accuracy comparison.

311 To measure accuracy of body angles from an angular measurement sensor-based approach, knee-included
312 angles directly obtained from an optical encoder were compared with the angles determined by 3D locations
313 of markers attached to hip, knee and ankle joints.

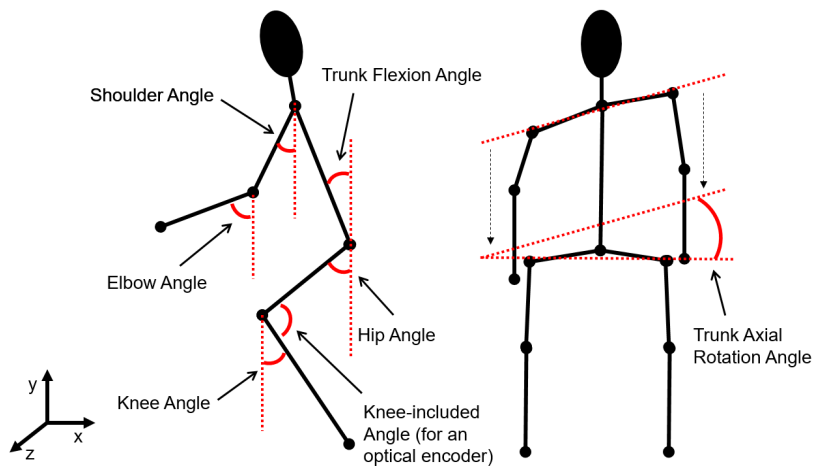


Figure 5. Body Angles to be Compared

314

315

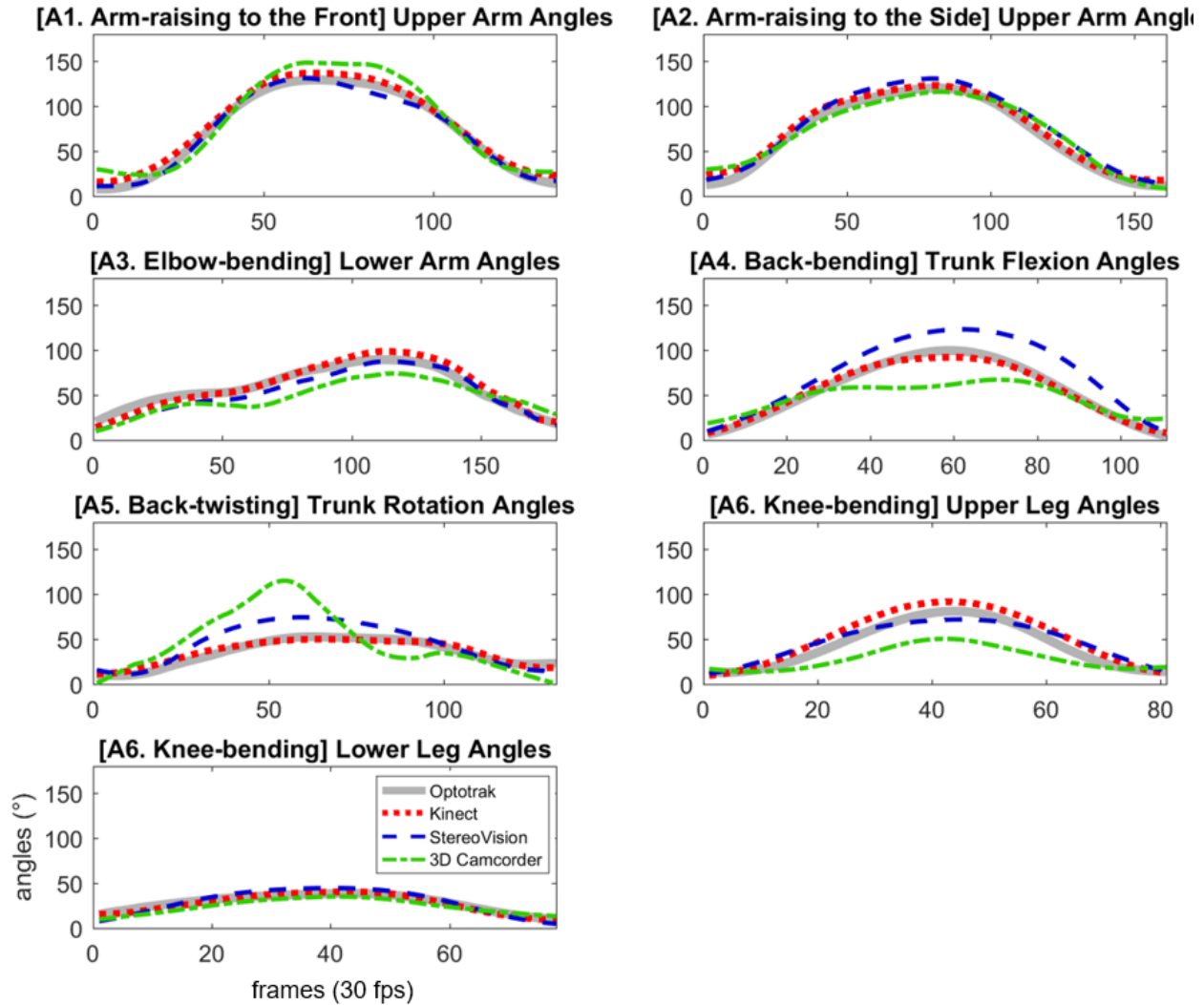
316

317 Ground truth body angles were calculated based on 3D marker positions from OptotrakTM. The markers
 318 were attached to the skin near the joints, not the centers of body joints. As a result, body angles from
 319 OptotrakTM may slightly differ from the angles from vision- and angular measurement sensor-based
 320 approaches. To adjust possible discrepancies, the body angles were calibrated using the angles from a T-
 321 pose. Also, the body angles from each approach were smoothed using a Savitzky–Golay filter [40] that has
 322 been widely used for post processing of motion data [41].

323 Results

324 Vision-based motion capture approaches

325 Figure 6 shows plots of body angles from vision-based motion capture approach during one cycle of diverse
 326 basic tasks. Through the visual investigation, it was found that overall body angles from each approach
 327 were closely matched with body angles from an OptotrakTM, while back (flexion and rotation) and upper
 328 leg angles from a multiple camera-based approach in particular showed some discrepancies during the
 329 middle of the tasks.



330

331

Figure 6. Comparison of Body Angles from Vision-based Approaches during Basic Tasks

332

333

For the quantitative assessment during these tasks, mean and standard deviation of absolute errors (MAEs

334

and S.D. of AEs), and maximum and minimum errors (MAX and MIN) in body angles between four

335

different approaches and an OptotrakTM were calculated as shown in Table 1. An RGB-D sensor-based

336

approach showed the most accurate (4.2 degrees of average MAEs) and reliable (2.8 degrees of average

337

S.D.) results for all body angles. A stereovision camera-based approach also provided relatively accurate

338

motion data, resulting in 6.2 degrees of MAE, but showed higher variations (4.2 degrees of average S.D.)

339

than an RGB-D sensor-based approach. The least accurate results (11.6 degrees of average MAEs) were

340

obtained from a multiple camera-based approach, especially due to relatively larger errors in lower arm

341 (16.2 degrees of MAEs), truck flexion (12.5 degrees of MAEs) and trunk rotation (21.9 degrees of MAEs)
 342 angles than other body angles.

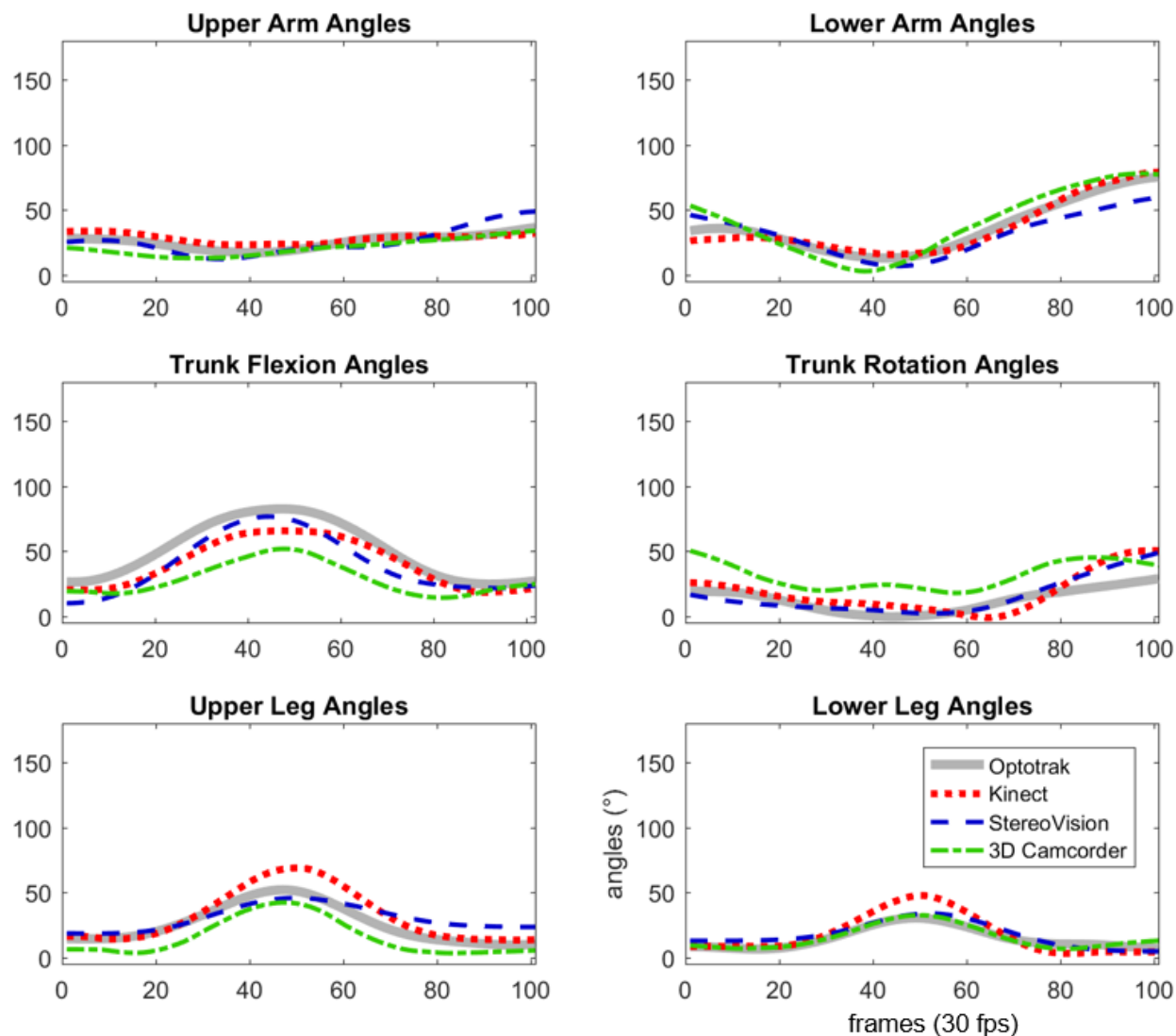
343 Table 1. Accuracy of Body Angles from Vision-based Approaches during Basic Tasks
 344 (Unit: degrees)

| Body Angles | Metrics | RGB-D Sensor (Kinect™) | Stereovision Camera (Bumblebee XB3™) | Multiple Camera (3D Camcorder) |
|-------------------------------------|------------|---------------------------|---|---|
| A1. Arm-raising to the front | | | | |
| Upper Arm | MAE | 5.9 | 3.0 | 11.3 |
| | S.D. of AE | 2.5 | 2.6 | 6.8 |
| | MIN/MAX | -9.9 to -0.6 | -3.2 to 9.9 | -22.0 to 12.0 |
| A2. Arm-raising to the side | | | | |
| Upper Arm | MAE | 4.7 | 8.2 | 7.6 |
| | S.D. of AE | 2.3 | 3.8 | 4.2 |
| | MIN/MAX | -11.1 to -1.9 | -14.3 to -0.3 | -16.8 to 7.6 |
| A3. Elbow-bending | | | | |
| Lower Arm | MAE | 4.9 | 8.1 | 16.2 |
| | S.D. of AE | 3.4 | 4.0 | 4.2 |
| | MIN/MAX | -9.8 to 8.6 | -2.7 to 14.0 | 10.1 to 24.5 |
| A4. Back-bending | | | | |
| Back Flexion | MAE | 2.5 | 15.5 | 12.5 |
| | S.D. of AE | 2.1 | 11.2 | 12.5 |
| | MIN/MAX | 7.6 | 0.0 | 39.0 |
| | MIN | -3.9 | -34.3 | -19.7 |
| A5. Back-twisting | | | | |
| Back Axial Rotation | MAE | 3.1 | 11.0 | 21.9 |
| | S.D. of AE | 1.9 | 8.6 | 18.5 |
| | MIN/MAX | -6.5 to 4.6 | -23.8 to 8.6 | -64.6 to 22.5 |
| A6. Knee-bending | | | | |
| Upper Leg | MAE | 5.4 | 4.3 | 9.8 |
| | S.D. of AE | 5.5 | 4.6 | 12.0 |
| | MIN/MAX | -13.7 to 3.3 | -14.0 to 9.3 | -4.9 to 32.4 |
| Lower Leg | MAE | 1.0 | 2.4 | 2.7 |
| | S.D. of AE | 1.1 | 2.6 | 2.8 |
| | MIN/MAX | -1.7 to 4.1 | -6.5 to 7.6 | -3.3 to 8.1 |
| Average MAE | | 4.2 | 6.2 | 11.6 |
| Average S.D. | | 2.8 | 4.4 | 8.1 |

345 Notes: MAE (Mean Absolute Error), AE (Absolute Error), S.D. (Standard Deviation), MAX (Maximum Value of
 346 Errors), MIN (Minimum Value of Errors)

347
 348 Figure 7 shows body angles from vision-based approaches during one cycle of a lifting and placing task.
 349 Even for a complex task that involves simultaneous whole body movements, all the approaches provided

350 robust body angle measurements for all body parts. Unlike basic tasks, any severe discrepancies in body
 351 angles from a multiple camera-based approach were not observed.



352
 353 Figure 7. Comparison of Body Angles from Vision-based Approaches during a Lifting and Placing Task
 354

355 Average MAEs during a lifting and placing task were 6.5 (RGB-D sensor-based), 6.6 (stereovision camera-
 356 based), and 10.9 (multiple camera-based) degrees, showing similar errors in body angles during basic tasks
 357 (Table 2). Both RGB-D sensor- and stereovision camera-based approaches showed robust results in this
 358 task, even though errors in body angles in a RGB-D sensor-based approach were slightly increased. Again,

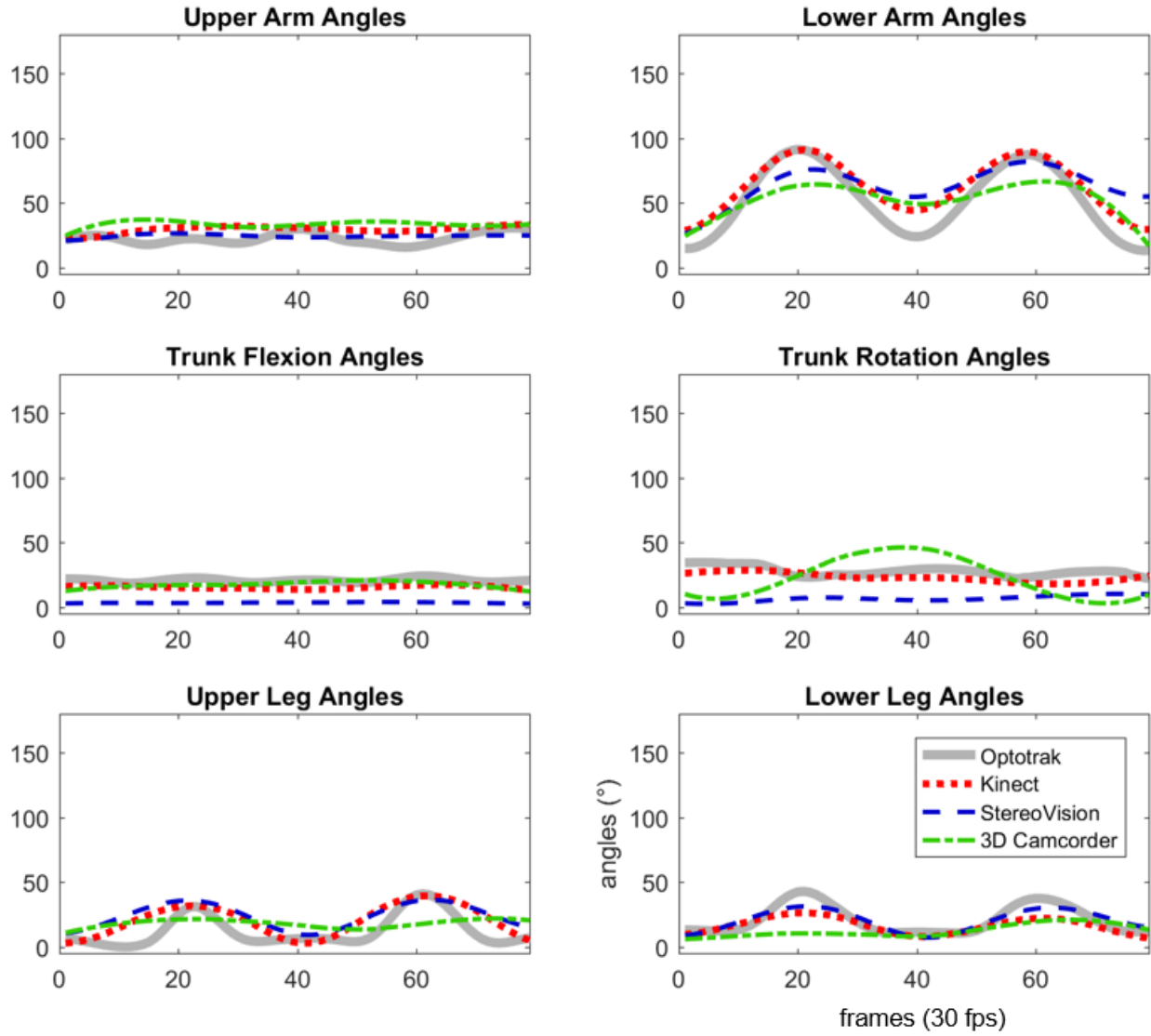
359 in motion data from a multiple camera-based approach, larger errors in back (torso flexion and rotation)
 360 angles were observed while upper arm angles were relatively accurate.

361 Table 2. Accuracy of Body Angles from Vision-based Approaches during a Lifting and Placing Task
 362 (Unit: degrees)

| Body Angles | Metrics | RGB-D Sensor (Kinect™) | Stereovision Camera (Bumblebee XB3™) | Multiple Camera (3D Camcorder) |
|------------------------|------------|---------------------------|---|-----------------------------------|
| Upper Arm | MAE | 3.5 | 4.6 | 4.4 |
| | S.D. of AE | 2.4 | 3.8 | 3.3 |
| | MIN/MAX | -6.3 to 4.4 | -13.1 to 6.5 | 0.3 to 10.4 |
| Lower Arm | MAE | 3.6 | 7.6 | 7.5 |
| | S.D. of AE | 1.9 | 4.7 | 3.6 |
| | MIN/MAX | -4.9 to 8.3 | -12.1 to 16.2 | -19.3 to 11.1 |
| Back Flexion | MAE | 10.3 | 11.0 | 22.7 |
| | S.D. of AE | 5.1 | 5.2 | 11.2 |
| | MIN/MAX | 2.9 to 16.9 | 3.1 to 18.4 | 2.2 to 35.5 |
| Back Axial Rotation | MAE | 8.4 | 5.5 | 18.8 |
| | S.D. of AE | 6.2 | 5.2 | 4.8 |
| | MIN/MAX | -23.4 to 11.3 | -20.0 to 7.2 | -31.1 to -10.5 |
| Upper Leg | MAE | 6.9 | 7.1 | 10.3 |
| | S.D. of AE | 6.2 | 4.7 | 2.7 |
| | MIN/MAX | -19.4 to 1.5 | -13.9 to 7.0 | 4.6 to 14.9 |
| Lower Leg | MAE | 6.0 | 4.0 | 1.5 |
| | S.D. of AE | 5.0 | 1.8 | 1.4 |
| | MIN/MAX | -17.5 to 7.2 | -6.7 to 4.0 | -6.1 to 3.7 |
| Average MAE | | 6.5 | 6.6 | 10.9 |
| Average S.D. | | 4.5 | 4.2 | 4.5 |

363 Notes: MAE (Mean Absolute Error), AE (Absolute Error), S.D. (Standard Deviation), MAX (Maximum Value of
 364 Errors), MIN (Minimum Value of Errors)

365
 366 Lastly, a walking task showed larger discrepancies in the patterns of body angles from all vision-based
 367 approaches as shown in Figure 8. Motion data from RGB-D sensor- and multiple camera-based approaches
 368 induced similar errors (7.1 and 11.0 degrees of average MAEs, respectively) with other tasks while a
 369 stereovision camera-based approach showed the largest errors (12.6 degrees of average MAEs) among three
 370 tasks (Table 3).



371

372 Figure 8. Comparison of Body Angles from Vision-based Approaches during a Walking Task

373

374
375

Table 3. Accuracy of Vision-based Motion Capture Approaches during a Walking Task
(Unit: degrees)

| Body Angles | Metrics | RGB-D Sensor (Kinect™) | Stereovision Camera (Bumblebee XB3™) | Multiple Camera (3D Camcorder) |
|------------------------|------------|---------------------------|---|--------------------------------------|
| Upper Arm | MAE | 7.1 | 4.5 | 10.9 |
| | S.D. of AE | 4.0 | 2.3 | 5.5 |
| | MIN/MAX | -13.3 to 1.8 | -8.7 to 6.5 | -19.3 to -2.0 |
| Lower Arm | MAE | 10.7 | 15.9 | 15.0 |
| | S.D. of AE | 6.3 | 11.6 | 7.7 |
| | MIN/MAX | -20.6 to 1.1 | -41.8 to 17.1 | -25.4 to 28.0 |
| Back Flexion | MAE | 5.4 | 17.3 | 3.5 |
| | S.D. of AE | 1.5 | 1.4 | 2.2 |
| | MIN/MAX | 2.3 to 7.9 | 15.0 to 20.4 | -1.7 to 9.4 |
| Back Axial Rotation | MAE | 4.8 | 21.3 | 15.3 |
| | S.D. of AE | 4.8 | 5.3 | 8.1 |
| | MIN/MAX | -24.4 to 8.8 | 14.6 to 32.0 | -18.6 to 27.9 |
| Upper Leg | MAE | 8.8 | 12.1 | 11.6 |
| | S.D. of AE | 6.6 | 7.2 | 5.5 |
| | MIN/MAX | -21.2 to 3.8 | -27.3 to 4.9 | -18.9 to 23.1 |
| Lower Leg | MAE | 5.6 | 4.2 | 9.7 |
| | S.D. of AE | 5.1 | 2.7 | 8.9 |
| | MIN/MAX | -4.3 to 16.6 | -6.9 to 11.6 | -5.0 to 32.5 |
| Average MAE | | 7.1 | 12.6 | 11.0 |
| Average S.D. | | 4.7 | 5.9 | 6.3 |

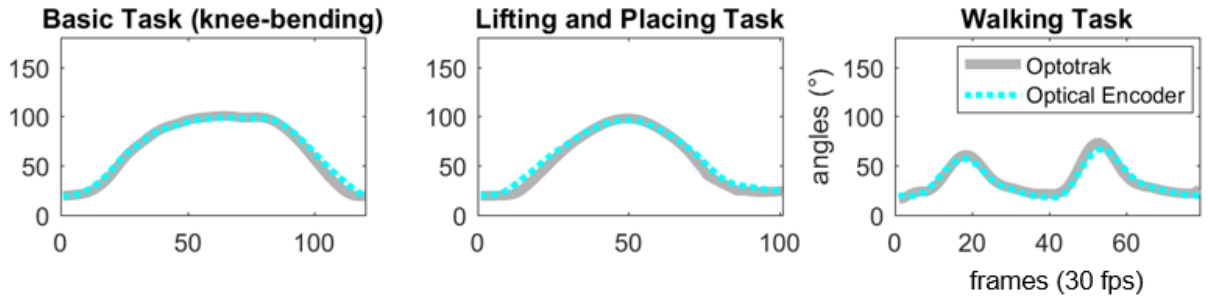
376
377
378

Notes: MAE (Mean Absolute Error), AE (Absolute Error), S.D. (Standard Deviation), MAX (Maximum Value of Errors), MIN (Minimum Value of Errors)

379 *An angular measurement sensor-based approach*

380 Figure 9 shows plots of knee-included angles measured using an optical encoder and an Optotak™ during
381 three tasks (among basic tasks, only the knee-bending task was tested). Two plots were almost matched
382 each other, indicating accurate angular measurement of an optical encoder for all three tasks. However,
383 small discrepancies were observed at the beginning and end of the cycle of knee-bending, and lifting and
384 placing tasks.

385



386

387

388

Figure 9. Comparison of Knee-included Angles from an Angular Measurement Sensor-based Approach (i.e., an optical encoder) during three tasks

389

390

391

392

393

A MAE for knee-included angles from an optical encoder was 2.9, 3.8 and 3.0 degrees for three tasks, respectively (Table 4). Compared with a RGB-D sensor-based approach that showed the most accurate measurements for upper and lower leg angles (1.0–8.8 degrees of MAEs) among vision-based approaches, this approach provided the most accurate and reliable angular measurements regardless of types of tasks.

394

395

396

Table 4. Accuracy of an Angular Measurement Sensor-based Approach (i.e., an optical encoder) during Three Tasks

| | | (Unit: degrees) | | |
|---------------|------------|-----------------|--------------------------|--------------|
| Body Angles | Metrics | Basic Task | Lifting and Placing Task | Walking Task |
| Knee-included | MAE | 2.9 | 3.8 | 3.0 |
| | S.D. of AE | 2.7 | 3.1 | 2.1 |
| | MIN/MAX | -10.1 to 2.0 | -10.7 to 1.8 | -5.6 to 8.8 |

397

398

399

Notes: MAE (Mean Absolute Error), AE (Absolute Error), S.D. (Standard Deviation), MAX (Maximum Value of Errors), MIN (Minimum Value of Errors)

400

DISCUSSION

401

Performance Comparison

402

403

404

405

Specifications and accuracies of three vision-based motion capture approaches and an optical encoder are summarized in Table 5. The experimental tests in the previous section presented 5.9, 8.5, 11.2 and 3.2 degrees of average MAEs for RGB-D sensor-based, stereovision camera-based and multiple camera-based approaches, and an optical encoder, respectively. The motion capture performance of each approach tends

406 to rely on the specifications of devices (e.g., types of raw data, resolution, fps). For better decisions on
 407 appropriate uses of these approaches in construction, it would be important not only to compare the
 408 accuracy, but also to understand comparative advantages and limitations.

409 Table 5. Comparison of Specifications and Accuracies of Vision-based Motion Capture Approaches

| Performance | | RGB-D Sensor (Kinect™) | Stereovision Camera (Bumblebee XB3™) | Multiple Camera (3D Camcorder) | Optical Encoder |
|---------------------|------------------------|-----------------------------------|---|---|----------------------------|
| Specifica- tions | Raw Data | 3D images | 3D images | 2D images | Body angles |
| | Operating Range | Less than 4m | Less than 10 m (unlimited, with zoom lenses) | Unlimited with zoom lenses | Unlimited |
| | Resolution | 640×480 | 320×240 | 1920×1080 | - |
| | fps | 30 | 8-10 | 29 | 550 |
| Accuracy (MAEs) | Basic Tasks | 4.2° | 6.2° | 11.6° | 2.9° |
| | Lifting and Placing | 6.5° | 6.6° | 10.9° | 3.8° |
| | Walking | 7.1° | 12.6° | 11.0° | 3.0° |
| | Average | 5.9° | 8.5° | 11.2° | 3.2° |

410
 411 Among vision-based approaches, an RGB-D sensor-based approach showed the most accurate and reliable
 412 results for all three tasks as it uses data-rich 3D images and has a high resolution and frame rate. It is also
 413 expected that rapid technological development of RGB-D sensors will enable us to collect more accurate
 414 and reliable 3D point cloud data, contributing to improvement of motion tracking performance. Despite the
 415 robust performance of this approach, its short operating range (less than 4m) and sensitivity to sunlight may
 416 limit its application to confined and indoor areas.

417 Alternatively, a stereovision camera-based approach can be a practical solution by taking advantage of its
 418 ability to collect 3D images at both indoor and outdoor conditions and longer operating range. The accuracy
 419 of body angles from this approach was also not much different from RGB-D sensor-based approach, when
 420 excluding the walking task. Considering that walking involves more rapid movements than other tasks in
 421 this test, it was likely that the low frame rate (8-10 fps) of the stereovision resulted in tracking errors of

422 certain body parts (e.g., upper limbs) that moved quickly. As the frame rate of a stereovision camera is
423 determined by the computational time for 3D reconstruction and the performance of hardware, the use of
424 an advanced 3D reconstruction algorithm and a high performance computer can achieve a higher frame rate
425 that helps to reduce errors in motion data, particularly during tasks involving rapid body movements.
426 Regarding the operating range of a stereovision camera-based approach, it is recommended to set a
427 Bumblebee XB3™ within 10 m as the quality of 3D point clouds is significantly affected by the distance
428 from the scene. However, a binocular stereovision system theoretically works with any type of two 2D
429 cameras that are separated by a short distance, and are mounted parallel to one another. As a result, this
430 approach is flexible in terms of operating ranges if zoom lenses are used. Recently, a stereovision system
431 with adjustable zoom lens control has been introduced [42], enabling more practical application of this
432 approach.

433 A multiple camera-based approach showed larger errors in body angles than the other two vision-based
434 approaches. RGB-D sensor-based and stereovision camera-based approaches benefit from 3D imaging
435 hardware that provides richer information (e.g., RGB pixel values + depth information) on scenes. However,
436 a multiple camera-based approach need to extract motion data by processing only 2D images that contain
437 less information (e.g., RGB pixel values). Inaccurate camera calibration process could also lead to errors in
438 3D triangulation of body joints from two images. Considering these limitations, a multiple camera-based
439 approach with about 10 degrees of error in body angles is promising. Despite relatively larger errors, a
440 multiple camera-based approach has several competitive advantages from a practical point of view,
441 compared with the other two approaches. For example, as any types of ordinary cameras can be used to
442 collect 2D images, additional investments in devices are not required. Due to the use of zoom lenses, its
443 operating range is theoretically unlimited. Less sensitivity to rapid movements is another strength of this
444 approach. In addition, there is room for further improvement if occlusion issues are handled. One of the
445 reasons of the least accurate results from a multiple camera-based approach is that it showed relatively
446 larger errors in lower arm, truck flexion and trunk rotation angles than other body angles. As shown in A3

447 (elbow-bending), A4 (back-bending) and A5 (back-twisting) tasks in Figure 4, an elbow or a hip was
448 occluded by a lower arm or a torso (i.e., self-occlusions), which may lead to incorrect detections of these
449 joints in a multiple camera-based approach. In these tests, especially, a 3D camcorder was used to obtain
450 two images from different views. As the distance between two lenses is very short (3.5 cm), both images
451 are affected by self-occlusions. If two independent cameras are positioned away from each other, it could
452 be possible to obtain at least one clear view of images, reducing errors due to self-occlusions.

453 The optical encoder provided quite accurate measurements for knee-included angles across all types of
454 tasks. Further, as these sensors are attached to body joints to directly measure joint angles, they can provide
455 robust angular measurements for body joints with one degree of freedom under any condition. Although
456 angular measurement sensors, such as, the optical encoder can be used for all body joints, the use of these
457 sensors could be limited due to the need for straps or exoskeletons that may lead to interfering with on-
458 going work. Instead, using angular measurement sensor-based approaches for selected body joints can
459 offset the limitation of vision-based approaches that are sensitive to self-occlusions. However, soft tissue
460 movements may result in errors in body angles from these sensors. For example, during the testing of this
461 approach, small differences in knee-included angles were observed at the beginning and end of cycles,
462 which can be attributed to soft tissue movements, especially when straps are not firmly secured to the leg.
463 Securing straps firmly to the body to hold the sensor in position is an important factor to obtain accurate
464 body angles from the sensor [43].

465 **Potential Application Areas of In-field Motion Capture Approaches in Construction**

466 Vision- and angular measurement sensor-based motion capture approaches tested in this study are
467 considered practical means of in-field motion capture, even though about 5-10 degrees of error in body
468 angles from vision-based approaches and about 3 degrees of error from an angular measurement sensor-
469 based approach still exist. In construction, tasks are performed in unstructured and varying environments,
470 and thus work methods and postures are changing over time. Collecting motion data using these non-

471 invasive and cost effective approaches enable us to understand how workers interact with the environment
472 at construction sites and to identify potential safety and health risks under given environments, specifically
473 when accuracies would not significantly matter such as rough postural assessment, time and motion study,
474 and trajectory analysis.

475 For example, these approaches can be used to specify the severity of working postures. Existing postural
476 ergonomic risk assessment methods determine the level of ergonomic risks based on classified postures
477 through human observation [44]. Some methods such as Rapid Upper Limb Assessment (RULA) [45] and
478 Rapid Entire Body Assessment (REBA) [46] require detailed segmentations of body postures according to
479 body angles. For example, in RULA, trunk postures are categorized into four groups according to trunk
480 flexion angles (0° , 0° - 20° , 20° - 60° and over 60°). Body angles obtained from these approaches can be used
481 for rough posture classification that is needed for postural risk assessments. Also, as continuously measured
482 workers' motions during performing tasks is enabled, diverse in-depth motion analysis for understanding
483 physical demands can be facilitated. Traditionally, pre-determined-motion-time-systems have been widely
484 used to identify workloads during occupational tasks [47]. As these systems rely on human observations to
485 describe workers' manual activities, significant human efforts are generally required. However, by using a
486 time series motion data from the presented approaches, it is possible to accurately and automatically
487 quantify motion-time values for these system. In addition, trajectory analysis through in-field motion
488 measurements helps to evaluate work efficiency, as well as the risk of ergonomic injuries. For example,
489 shorter trajectories of body movements may imply more efficient movements of a human body, indicating
490 smaller physical demands. Previous studies on movement patterns during occupational tasks found that a
491 more 'dynamic' pattern of movements is believed to be associated with a lower incidence of WMSD
492 development [48,49]. Analysis of motion patterns and trajectories using vision-based motion data can
493 broaden our understanding on the job from an ergonomic perspective.

494 In-field kinematic measurement using vision- and angular measurement sensor-based motion capture
495 approaches has also great potential to be used for more in-depth analysis of physical demands such as

496 biomechanical analysis, even though further improvement of motion data accuracy is required [50].
497 Biomechanical analysis aims to estimate musculoskeletal stresses as a function of motion and external force
498 data [4, 51]. Previous biomechanical studies have relied on laboratory experiments to collect motion data
499 using marker-based motion capture approaches, which can be replaced by in-field motion capture
500 approaches that enable on-site biomechanical analysis. As accurate measurement of all joint angles is
501 necessary for reliable biomechanical analysis, further accuracy improvement of vision-based motion
502 capture approaches is required. However, the sensitivity of biomechanical analysis results to motion errors
503 vary depending on body joints [52]. For example, Chaffin and Erig [52] found that an error of ± 10 degrees
504 in the limiting joint angles (e.g., knees and ankles) could cause the biomechanical analysis results to vary
505 up to $\pm 12\%$ during lifting, pushing and pulling tasks, whereas errors in other joints could have little or no
506 effect. This result indicates that some angular errors in body joints that do not involve forceful exertions
507 are acceptable for biomechanical analysis while it is important to obtain accurate body angles for stressful
508 body joints. So, complemented by relatively accurate angular measurement sensors such as optical encoders
509 that are applied to the limiting joints, vision-based motion capture approaches enable researchers to perform
510 biomechanical analysis without significantly sacrificing the reliability of biomechanical analysis.

511

512 **CONCLUSIONS**

513 The study describes the potential of vision-based and angular measurement sensor-based approaches as a
514 means of measuring workers' motions. These approaches are compared through laboratory tests while
515 performing three different types of tasks. Especially, the accuracy of these approaches was computed by
516 comparing body angles from each approach and a marker-based motion capture. The comparison results
517 indicated that the overall errors in body angles from vision-based approaches are about more or less 10
518 degrees, while an optical encoder that is one example of angular measurement sensors can provide quite

519 accurate body angle measurements (about 3 degrees) for specific body joints with one degree of freedom.
520 Self-occlusions and rapid movements are major factors that lead to errors in vision-based approaches.

521 From a practical perspective, vision-based and angular measurement sensor-based approaches have great
522 potential as non-invasive motion data collection methods at construction sites. Even though several
523 obstacles such a limited operating range (RGB-D sensor-based), low frame rates (stereovision camera) and
524 occlusions (multiple camera-based) still remain to obtain more accurate data from these approaches, further
525 algorithm refinements and hardware developments are expected to address these issues. An angular
526 measurement sensor-based approach such as an optical encoder can provide robust measurements of
527 specific joint movements, despite a small possibility of discomfort by attached sensors. Especially,
528 combined with vision-based motion capture approaches, an angular measurement sensor-based approach
529 can enhance the accuracy of in-field motion measurements. Motion data from these approaches can be used
530 for diverse in-depth analysis without sacrificing its reliability to better understand workers' physical
531 demands during occupational tasks including construction. Also, understanding of how workers behave
532 under given working environments through kinematics measurements and analysis helps to ergonomically
533 design automated machines and assistive robots, aiming to both reduce physical demands and enhance
534 workers' capabilities.

535

536 **ACKNOWLEDGEMENT**

537 The work presented in this paper was supported with a National Science Foundation Award (No. IIP
538 1640633) in United States, and was partially supported by a grant from the Research Grants Council of the
539 Hong Kong Special Administrative Region, China (Project No. PolyU 25210917). Any opinions, findings,
540 and conclusions or recommendations expressed in this paper are those of the authors and do not necessarily
541 reflect the views of the National Science Foundation and the Research Grants Council.

542

544 **REFERENCES**

- 545 [1] J.G. Everett, “Overexertion injuries in construction,” *J. Constr. Eng. Manag.* 125(2), 109–114 (1999).
- 546 [2] Center for Construction Research and Training (CPWR), The construction chart book: The U.S.
547 construction industry and its workers (CPWR Publications. Silver Spring, MD, USA, 2013).
- 548 [3] V.M. Zatsiorski, Kinematics of human motion (Human Kinetics. Champaign, IL, USA, 2002).
- 549 [4] R.G. Radwin, W.S. Marras and S.A. Lavender, “Biomechanical aspects of work-related
550 musculoskeletal disorders,” *Theor. Issues Ergon.* 2(2), 153–217 (2001).
- 551 [5] T.J. Armstrong, P. Buckle, L.J. Fine, M. Hagberg, B. Jonsson, A. Kilbom, ... and E.R. Viikari-Juntura,
552 “A conceptual model for work-related neck and upper-limb musculoskeletal disorders,” *Scand. J.*
553 *Work Environ. Health*, 19(2), 73–84 (1993).
- 554 [6] J.G. Everett and A.H. Slocum, “Automation and robotics opportunities: construction versus
555 manufacturing,” *J. Constr. Eng. Manag.* 120(2), 443–452 (1994).
- 556 [7] A. Schiele and F.C. van der Helm, “Kinematic design to improve ergonomics in human machine
557 interaction,” *IEEE Trans. Neural Syst. Rehabil. Eng.* 14(4), 456–469 (2006).
- 558 [8] K. Aminian, and B. Najafi, “Capturing human motion using body-fixed sensors: outdoor measurement
559 and clinical applications,” *Comput. Animat. Virtual Worlds*, 15(2), 79–94 (2004).
- 560 [9] T. Takubo, Y. Imada, K. Ohara, Y. Mae and T. Arai, “Rough terrain walking for bipedal robot by
561 using ZMP criteria map,” *Proceedings of the 2009 IEEE International Conference on Robotics and*
562 *Automation*, (May 12-17, 2009) pp. 788–793.
- 563 [10] S.R. Cruz-Ramírez, Y. Mae, T. Arai, T. Takubo and K. Ohara, “Vision-based hierarchical recognition
564 for dismantling robot applied to interior renewal of buildings.” *Comput. Aided Civ. Inf.* 26(5), 336–
565 355 (2011).
- 566 [11] T. Jacobs, U. Reiser, M. Hägele and A. Verl, “Development of validation methods for the safety of
567 mobile service robots with manipulator.” *Proceedings of the 7th German Conference on Robotics*
568 *(ROBOTIK)*, Munich, Germany, (May 21-22, 2012) pp. 117–122.

- 569 [12] G. Migliaccio, J. Teizer, T. Cheng and U. Gatti, “Automatic identification of unsafe bending behavior
570 of construction workers using real-time location sensing and physiological status monitoring,”
571 *Proceedings of the Construction Research Congress (CRC)*, West Lafayette, IN, USA (May 21-23,
572 2012).
- 573 [13] S.J. Ray and J. Teizer, “Real-time construction worker posture analysis for ergonomics training,” *Adv.*
574 *Eng. Inform.* 26(2), 439–455 (2012).
- 575 [14] C. Georgoulas, T. Linner and T. Bock, “Towards a vision controlled robotic home environment,”
576 *Automat. Constr.* 39, 106–116 (2014).
- 577 [15] T. Linner, J. Güttler, T. Bock and C. Georgoulas, “Assistive robotic micro-rooms for independent
578 living,” *Automat. Constr.* 51, 8–22 (2015).
- 579 [16] S. Han and S. Lee, “A vision-based motion capture and recognition framework for behavior-based
580 safety management,” *Automat. Constr.* 35, 131–141 (2013).
- 581 [17] S. Han, M. Achar, S. Lee and F. Peña-Mora, “Empirical assessment of a RGB-D sensor on motion
582 capture and action recognition for construction worker monitoring,” *Visualization in Engineering* 1(1),
583 1–13 (2013).
- 584 [18] M. Liu, S. Han and S. Lee, “Tracking-based 3D human skeleton extraction from stereo video camera
585 toward an on-site safety and ergonomic analysis,” *Construction Innovation* 16(3) (2016).
- 586 [19] R. Starbuck, J. Seo, S. Han and S. Lee, “A stereo vision-based approach to marker-less motion capture
587 for on-site kinematic modeling of construction worker tasks.” *Proceedings of the 15th International*
588 *Conference on Computing in Civil and Building Engineering (ICCCBE)*, Orlando, FL, USA (June 23-
589 25, 2014).
- 590 [20] A.A. Alwasel, K. Elrayes, E.M. Abdel-Rahman, and C.T. Haas, “A human body posture sensor for
591 monitoring and diagnosing MSD risk factors,” *Proceedings of the 30th International Symposium on*
592 *Automation and Robotics in Construction (ISARC)*, Montreal, Canada (Aug, 11–15, 2013).
- 593 [21] R. Poppe, “A survey on vision-based human action recognition,” *Image Vision Comput.* 28(6), 976–
594 990 (2010).

- 595 [22] M.W. Lee and I. Cohen, "A model-based approach for estimating human 3D poses in static images,"
596 *IEEE T. Pattern Anal.* 28(6), 905–916 (2006).
- 597 [23] C. Plagemann, V. Ganapathi, D. Koller and S. Thrun, "Real-time identification and localization of
598 body parts from depth images," *Proceedings of the 2010 IEEE International Conference on Robotics
599 and Automation (ICRA)*, Anchorage, AK, USA (2010) pp. 3108–3113.
- 600 [24] M. Siddiqui and G. Medioni, "Human pose estimation from a single view point, real-time range sensor,"
601 *Proceedings of the 2010 IEEE Computer Society Conference on Computer Vision and Pattern
602 Recognition Workshops (CVPRW)*, San Francisco, CA, USA (June 13-18, 2010) pp. 1–8.
- 603 [25] J. Shotton, T. Sharp, A. Kipman, A. Fitzgibbon, M. Finocchio, A. Blake and R. Moore, "Real-time
604 human pose recognition in parts from single depth images." *Commun. ACM* 56(1), 116–124 (2013).
- 605 [26] N. Rafibakhsh, J. Gong, M.K. Siddiqui, C. Gordon and H.F. Lee, "Analysis of xbox kinect sensor data
606 for use on construction sites: depth accuracy and sensor interference assessment," *Proceedings of
607 Constitution Research Congress (CRC)*, West Lafayette, IN, USA (May 21-23, 2012) pp. 848–857.
- 608 [27] Z. Zhang, "Microsoft kinect sensor and its effect." *IEEE Multimedia Mag.* 19(2), 4–10 (2012).
- 609 [28] S. Jin, J. Cho, X.D. Pham, K.M. Lee, S.K. Park, M. Kim and J.W. Jeon, "FPGA design and
610 implementation of a real-time stereo vision system," *IEEE T. Circ. Syst. Vid.* 20(1), 15–26 (2010).
- 611 [29] J.I. Woodfill, G. Gordon and R. Buck, "Tyzx deepsea high speed stereo vision system," *Proceedings
612 of the Conference on Computer Vision and Pattern Recognition Workshop (CVPRW'04.)* Washington,
613 DC, USA, (June 27-July 2, 2004).
- 614 [30] C. Shan, T. Tan and Y. Wei, "Real-time hand tracking using a mean shift embedded particle filter,"
615 *Pattern Recogn.* 40(7), 1958–1970 (2007).
- 616 [31] C. Liu, J. Yuen and A. Torralba, "SIFT flow: Dense correspondence across scenes and its
617 applications," *IEEE T. Pattern Anal.* 33(5), 978–994 (2011).
- 618 [32] J.R.R. Uijlings, A.W.M. Smeulders and R.J.H. Scha, "Real-time visual concept classification," *IEEE
619 Trans. Multimedia* 12(7), 665–681 (2010).

- 620 [33] H. Bay, T. Tuytelaars and L. van Gool, "SURF: Speeded up robust features", *Comput. Vis. Image*
621 *Underst.* 110(3), 346–359 (2008).
- 622 [34] R. Hartley and A. Zisserman, *Multiple view geometry in computer vision* (Cambridge university press.
623 Cambridge, UK, 2003)
- 624 [35] Z. Zhang, "A flexible new technique for camera calibration," *IEEE Trans. Pattern Anal. Mach. Intell.*
625 22(11), 1330–1334 (2000).
- 626 [36] M. Tousignant, L. de Bellefeuille, S. O'Donoghue and S. Grahovac, "Criterion validity of the cervical
627 range of motion (CROM) goniometer for cervical flexion and extension." *Spine* 25(3), 324–330 (2000).
- 628 [37] A.A. Alwasel, E.M. Abdel-Rahman and C.T. Haas, "A technique to detect fatigue in the lower limbs,"
629 *Proceedings of the ASME 2014 International Design Engineering Technical Conferences and*
630 *Computers and Information in Engineering Conference*, New York, USA (Aug. 17–20, 2014)
- 631 [38] T. Yamada, Y. Hayamizu, Y. Yamamoto, Y. Yomogida, A. Izadi-Najafabadi, D.N. Futaba and K. Hata,
632 "A stretchable carbon nanotube strain sensor for human-motion detection," *Nat. Nanotechnol.* 6(5),
633 296–301 (2011).
- 634 [39] P.H. Veltink, H.B. Bussmann, W. De Vries, W.L. Martens and R.C. Van Lummel, "Detection of static
635 and dynamic activities using uniaxial accelerometers," *IEEE Trans. Neural Syst. Rehabil. Eng.* 4(4),
636 375–385 (1996).
- 637 [40] A. Savitzky and M.J. Golay, "Smoothing and differentiation of data by simplified least squares
638 procedures," *J. Anal. Chem.* 36(8), 1627–1639 (1964).
- 639 [41] P. Esser, H. Dawes, J. Collett and K. Howells, "IMU: inertial sensing of vertical CoM movement." *J.*
640 *Biomech.* 42(10), 1578–1581 (2009).
- 641 [42] M.Y. Kim, S.M. Ayaz, J. Park and Y. Roh, "Adaptive 3D sensing system based on variable
642 magnification using stereo vision and structured light," *Opt. Laser Eng.* 55, 113–127 (2014).
- 643 [43] P.J. Rowe, C.M. Myles, S.J. Hillmann and M.E. Hazlewood, "Validation of flexible electrogoniometry
644 as a measure of joint kinematics." *J. Physiother.* 87(9), 479–488 (2001).

- 645 [44] G. Li and P. Buckle, "Current techniques for assessing physical exposure to work-related
646 musculoskeletal risks, with emphasis on posture-based methods," *Ergonomics* 42(5), 674–695 (1999).
- 647 [45] L. McAtamney and E.N. Corlett, "RULA: a survey method for the investigation of work-related upper
648 limb disorders." *Appl. Ergon.* 24(2), 91–99 (1993).
- 649 [46] S. Hignett and L. McAtamney, "Rapid entire body assessment (REBA)," *Appl. Ergon.* 31(2), 201–205
650 (2000).
- 651 [47] W. Laurig, F.M. Kühn and K.C. Schoo, "An approach to assessing motor workload in assembly tasks
652 by the use of predetermined-motion-time systems," *Appl. Ergon.* 16(2), 119–125 (1985).
- 653 [48] Å. Kilbom and J. Persson, "Work technique and its consequences for musculoskeletal disorders,"
654 *Ergonomics*, 30(2), 273–279 (1987).
- 655 [49] Å Kilbom, "Repetitive work of the upper extremity: part II—the scientific basis (knowledge base) for
656 the guide," *Int. J. Ind. Ergon.* 14(1), 59–86 (1994).
- 657 [50] J. Seo, R. Starbuck, S. Han, S. Lee and T. Armstrong, "Motion-data-driven biomechanical analysis
658 during construction tasks on sites" *J. Comput. Civil Eng.* 29(4) (2014).
- 659 [51] D.B. Chaffin, G. Andersson and B.J. Martin, *Occupational Biomechanics* (4th edition). (Wiley. New
660 York, USA, 2006).
- 661 [52] D.B. Chaffin and M. Erig, "Three-dimensional biomechanical static strength prediction model
662 sensitivity to postural and anthropometric inaccuracies," *IIE Trans.* 23(3), 215–227 (1991).
- 663 [53] S. Knoop, S. Vacek and R. Dillmann, "Sensor fusion for 3D human body tracking with an articulated
664 3D body model," *Proceedings 2006 IEEE International Conference on Robotics and Automation, 2006*
665 *(ICRA 2006)*, 1686-1691 (2006).

| | | |
|-----|--|-----|
| 666 | Figure 1. RGB-D Sensor (i.e., Kinect™)-based Motion Capture | 6 |
| 667 | Figure 2. An Overview of a Multiple Camera-based Motion Capture Approach..... | 9 |
| 668 | Figure 3. Experimental Settings and Testing Devices | 13 |
| 669 | Figure 4. Testing Tasks..... | 14 |
| 670 | Figure 5. Body Angles to be Compared..... | 16 |
| 671 | Figure 6. Comparison of Body Angles from Vision-based Approaches during Basic Tasks | 17 |
| 672 | Figure 7. Comparison of Body Angles from Vision-based Approaches during a Lifting and Placing Task | |
| 673 | | 19 |
| 674 | Figure 8. Comparison of Body Angles from Vision-based Approaches during a Walking Task..... | 21 |
| 675 | Figure 9. Comparison of Knee-included Angles from an Angular Measurement Sensor-based Approach | |
| 676 | (i.e., an optical encoder) during three tasks | 233 |